The bulk osteosarcoma and osteosarcoma stem cell activity of a necroptosis-inducing nickel(II)-phenanthroline complex

Arvin Eskandari,[a]‡ Marie Flamme,[b]‡ Zhiyin Xiao,[c] and Kogularamanan Suntharalingam*[c]

Dedication ((optional))

[a] A. Eskandari
School of Pharmacy
University College London
London, UK
[b] M. Flamme
Department of Structural Biology and Chemistry
Institut Pasteur
Paris, France
[c] Dr Z. Xiao, Dr K. Suntharalingam
School of Chemistry
University of Leicester
Leicester, UK
E-mail: k.suntharalingam@leicester.ac.uk
‡ These authors contributed equally to this work

Supporting information for this article is given via a link at the end of the document.((Please delete this text if not appropriate))

Abstract: We report the anti-osteosarcoma and anti-osteosarcoma stem cell (OSC) properties of a nickel(II) complex, **1**. The nickel(II) complex, **1** displays similar potency towards bulk osteosarcoma cells and OSCs, in the micromolar range. Notably, **1** displays similar or better OSC potency than the clinically approved platinum(II) anticancer drugs, cisplatin and carboplatin, in two- and three-dimensional osteosarcoma cell cultures. Mechanistic studies revealed that **1** induces osteosarcoma cell death by necroptosis, an ordered form of necrosis. The nickel(II) complex, **1** triggers necrosome-dependent mitrochondrial membrane depolarisation and propidium iodide uptake. Interestingly, **1** does not evoke necroptosis by intracellular reactive oxygen species (ROS) elevation or poly ADP ribose polymerase (PARP-1) hyperactivation. ROS elevation and PARP-1 activity are traits that have been observed for established necroptosis-inducers such as shikinon, TRAIL, and glutamate. Thus the necroptosis pathway evoked by **1** is distinct. To the best of our awareness this is the first report into the anti-osteosarcoma and anti-OSC properties of a nickel complex.

Introduction

There are four main types of primary bone cancer that affect humankind; osteosarcoma, Ewing sarcoma, chondrosarcoma, and chordoma.[1] Of the four main types of primary bone cancer, osteosarcoma is the most widespread amongst adults and children.[2] The 5-year survival rate for osteosarcoma patients is 77% when the cancer is localised, however, the survival rate drops sharply to 22% when the tumour has spread to other parts of the body.[3] One of the reasons for the latter is the presence of osteosarcoma stem cells (OSCs).[4] OSCs are a small population of osteosarcomas with the ability to differentiate and self-renew.[5] OSCs divide slower than bulk osteosarcoma cells and thus can overcome traditional osteosarcoma-specific chemotherapeutics and radiation regimens which tend to target fast growing cells.[4a,6] OSCs, like cancer stem cells (CSCs) that originate from other tissues, have been heavily linked to the spread of tumours from a given primary site to distance organs.[7] The therapeutic arsenal currently available to oncologists is ineffective against OSCs at their therapeutically administered doses.[4a,6] Current therapeutic interventions enrich OSC populations by killing the bulk of osteosarcoma cells and leaving OSCs untouched, therefore increasing the likelihood of metastasis. Given our understanding of OSCs and its clinical implications, it is essential to develop novel treatments such as chemotherapeutic agents, which can remove whole osteosarcoma populations, including OSCs. The development of OSC-active chemotherapeutic agents is rare and has almost exclusively focused on organic compounds.[4a,8] Breast and glioma CSC-potent compounds containing metals have been recently developed by us and others.[9] We recently reported a series of gallium(III) complexes containing polypyridyl ligands with micromolar to nanomolar potency towards bulk osteosarcoma cells and OSCs (in monolayer and three-dimensional cell culture systems).[10] Mechanistic studies showed that the most effective gallium(III) complex in the series killed osteosarcoma cells, most probably, by inducing genomic DNA damage.[10]

Most metal complexes studied for their anticancer (and anti-CSC) activity are thought to trigger cell death by apoptosis, and thus are vulnerable to multi-drug resistance pathways.[11] More recently, a few inorganic compounds have also been shown to induce cell death via non-apoptotic pathways.[12] Biological studies have revealed and characterised a number of non-apoptotic pathways including autophagy, pyroptosis, ferroptosis, and necrosis.[13] Necrosis is a form of cell death that was first characterised as an unsystematic process with no regulation, however, more thorough investigations into this cell death pathway have uncovered that, it can in fact, proceed in a structured manner, in specific cells.[14] Necroptosis is a structured form of necrosis that has been widely studied and is

well-understood.[15] Necroptosis induction pivots on the formation of a protein complex referred to as the necrosome. The necrosome is made up of receptor-interacting protein kinase 1 (RIP1), receptor-interacting protein kinase 3 (RIP3), and the mixed lineage kinase domain-like protein (MLKL).[16] The necrosome facilitates cellular events that lead to necroptotic cell death, such as mitochondrial membrane depolarisation, plasma membrane permeabilisation, reactive oxygen species (ROS) elevation, and bioenergetics depletion.[16b,17] The necroptosis process uses protein machinery that is completely different from the execution proteins utilised in apoptosis, therefore, osteosarcoma cells that are intrinsically apoptosis resistant, could be vulnerable to chemical agents that can induce necroptosis.[18] Multi-drug resistant pathways (such as apoptosis resistance) are functional in OSCs.[4a,19] Given the above, necroptosis-inducers could theoretically be used to not only overcome apoptosis resistance in bulk osteosarcoma cells but also remove OSCs.

Osmium(II)- and ruthenium(II)-*p*-cymene complexes bearing bathophenanthroline and dichloroacetate ligands were recently reported to trigger necroptosis in breast CSCs.[20] The clinical success of anticancer platinum(II) drugs (cisplatin, carboplatin, and oxaliplatin)[21] has encouraged several studies into the application of other group 10 metal complexes, such as coordination nickel(II) complexes, as anti-bulk cancer cell agents.[22] Despite these investigations, little is known about the anti-CSCs properties of nickel-containing compounds. Nickel is more reactive than platinum and thus repurposing this reactivity to develop highly active anticancer agents with low general toxicity is a difficult task. In the context of anti-CSC nickel complexes, we reported a series of nickel(II) complexes containing phenanthroline and dithiocarbamate ligands capable of killing breast CSCs (and bulk breast cancer cells) in the micromolar range.[23] Mechanistic studies revealed that one of the nickel(II) complexes, [Ni(*N*,*N*-diethyldithiocarbamate)$_2$(1,10-phenanthroline)], **1** (Figure 1) killed breast CSCs by necroptosis.[23] Predictive functional genetic analysis, constructed on the basis of specific protein downregulation by RNA interference (RNAi), showed that the mode of cytotoxicity of the nickel(II) complex, **1** resembled shikonin, a well-studied necroptosis inducer.[23-24] Here, we report the potency of the necroptosis-inducing nickel(II)-phenanthroline-dithiocarbamate complex, **1** against OSCs and bulk osteosarcoma cells. Detailed mechanism of action studies on **1**-induced osteosarcoma cell death is also reported.

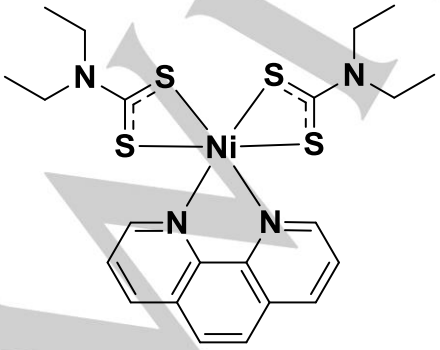

Figure 1. Chemical structure of the nickel(II) complex, [Ni(*N*,*N*-diethyldithiocarbamate)$_2$(1,10-phenanthroline)], **1** under investigation in this study. The nickel(II) complex is known to display micromolar potency towards bulk breast cancer cells and breast CSCs.

Results and Discussion

Bulk osteosarcoma and osteosarcoma stem cell potency

The nickel(II)-phenanthroline-dithiocarbamate complex, **1** (Figure 1) used in this work was prepared and characterized according to our previously reported protocol.[23] We used U2OS cells to determine the potency of **1** against bulk osteosarcoma cells and OSCs. U2OS cells are partially differentiated sarcoma-derived cells that can be easily handled in standard cell culture environments. Previous work has shown that when grown under standard cell culture conditions, U2OS cell populations typically comprise of *ca.* 1-4% OSCs.[25] The tyrosine kinase protein, CD117 is overexpressed on the cell surface of OSCs.[26] Using a previously reported method, we isolated OSC-enriched, CD117-positive cells by treating U2OS cells with methotrexate (300 nM) for 4 days.[10,25] This method allowed us to generate OSC-rich populations of U2OS cells, which we henceforth denote as U2OS-MTX cells.

The cytotoxicity of **1** towards U2OS and U2OS-MTX cells was assessed using the MTT [3-(4,5-dimethylthiazol-2-yl)-2,5-diphenyltetrazolium bromide] assay. IC_{50} values (concentration required to reduce cell viability by 50%) were derived from dose-response curves (Figure S1) and are summarised in Table 1. The nickel(II) complex, **1** exhibited very similar potency towards U2OS and U2OS-MTX cells in the micromolar range. The potency of **1** towards U2OS and U2OS-MTX cells was similar to, and in certain instances, significantly greater than the platinum(II) anticancer agents, cisplatin and carboplatin. Notably, salinomycin (an established CSC-active agent) displayed greater toxicity for U2OS and U2OS-MTX cells than **1** under identical conditions. The similarity in the cytotoxicity of **1** towards U2OS and U2OS-MTX cells implies that **1** could theoretically kill both bulk osteosarcoma and OSCs, in an *in vitro* setting, with a single micromolar dose. To determine therapeutic potential, the cytotoxicity of **1** towards non-cancerous HEK 293T embryonic kidney cells was determined. The complex, **1** was less potent toward HEK 293T cells (IC_{50} value = 35.0 ± 1.0 μM, Figure S2) than U2OS-MTX and U2OS cells, therefore **1** has the potential to remove osteosarcoma cells over non-cancerous kidney cells.

Table 1. IC_{50} values of the nickel(II)-phenanthroline-dithiocarbamate complex, **1**, cisplatin, carboplatin and salinomycin against U2OS and U2OS-MTX cells, and U2OS-MTX sarcospheres.

Compound	U2OS IC_{50} [μM] [a]	U2OS-MTX IC_{50} [μM] [a]	OSC-sarcosphere IC_{50} [μM] [a]
1	12.6 ± 1.2	10.8 ± 0.8	20.9 ± 1.9
cisplatin [b]	16.3 ± 0.5	33.9 ± 3.7	16.5 ± 0.2
carboplatin [b]	157.5 ± 2.2	115.0 ± 2.3	22.8 ± 0.1
salinomycin [b]	6.1 ± 1.1	1.5 ± 0.3	4.7 ± 0.1

[a] Determined after 3 or 10 days incubation (mean of three independent experiments ± SD). [b] Reported in reference 10.

Sarcospheres (three-dimensional spheroids) are solid tumour-like entities that can be generated when OSCs are cultured in non-adherent dishes or plates, with media lacking serum.[25] Given the three-dimensional nature of sarcospheres, they provide a reasonable model for assessing OSC potency

and the future *in vivo* prospects of a given chemical agent. The addition of **1** (IC_{20} values for 10 days) to individual cell suspensions of U2OS-MTX cells noticeably decreased the size of sarcospheres formed (Figure 2). Under the same conditions, cisplatin, carboplatin, or salinomycin (IC_{20} values for 10 days) was shown here, and previously, to have no major effect on the size of sarcospheres formed (Figure 2).[10] To determine the effect of **1** on sarcosphere viability, the resazurin-based indicator, TOX8 was employed. The nickel(II) complex, **1** exhibited micromolar activity towards sarcospheres (Table 1 and Figure S3), comparable to cisplatin and carboplatin (Table 1). Salinomycin exhibited greater sarcosphere potency than **1** under identical conditions (Table 1). Collectively, the standard cytotoxicity and sarcospheres studies indicate that **1** can kill OSCs at micromolar concentrations in both two-dimensional and three-dimensional osteosarcoma cell culture systems.

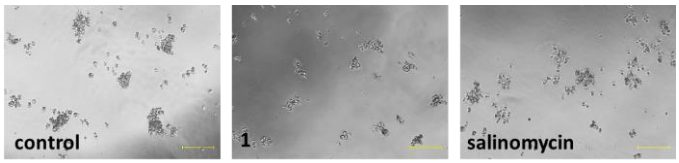

Figure 2. Representative bright-field images (× 10) of U2OS-MTX sarcospheres in the absence and presence of **1** or salinomycin at its IC_{20} value (10 days incubation). Scale bar = 100 µm.

Mode of cell death in osteosarcoma cells

Next, we probed the mode of cell death induced by **1** in osteosarcoma cells. The potency of **1** towards osteosarcoma cells was assessed upon co-treatment with necrosis and apoptosis inhibitors. Treatment of U2OS cells with **1** in the presence of IM-54 (10 µM), a potent inhibitor of oxidative stress-induced necrosis,[27] did not significantly change the potency of **1** ($p > 0.05$) towards U2OS cells (Figure 3, S4). This shows that **1**-induced osteosarcoma cell death is not related to unregulated necrosis. Necroptosis is an ordered form of necrosis, which is dependent on the assembly of necrosomes (made up of RIP1 and RIP3 kinases) that can instigate cell death.[15] The necroptosis signaling pathway is repressed by the RIP1 kinase inhibitor, necrostatin-1.[28] Co-treatment of **1** with necrostatin-1 (20 µM) significantly ($p < 0.05$) reduced the toxicity of **1** against U2OS cells (Figure 3, S4). The addition of shikonin, alone and in the presence of necrostatin-1 (20 µM), produced a similar effect to **1** without and with necrostatin-1 (Figure S5, S6). This suggests that **1** induces necrosome-dependent necroptosis in osteosarcoma cells. Immunoblotting studies indicated that RIP1 expression in U2OS cells markedly increased upon treatment with **1** (10-20 µM for 72 h; Figure S7). RIP3 (an essential necrosome component) is not expressed at clearly detectable levels in U2OS cells, however, treatment with **1** (10-20 µM for 72 h) noticeably increased RIP3 expression (Figure S7). Chemical-mediated restoration of RIP3 expression to detectable levels in RIP3 deficient cells is not unprecedented and has been previously observed for 5-aza-2'-deoxycytidine treatment.[29] Furthermore, shikinon dosage has been shown to induce RIP1 and RIP3 upregulation in U2OS cells, similar to **1**.[30] This suggests that **1**-induced necroptosis in osteosarcoma cells may be related to an increase in RIP1 and RIP3 expression, as well as their association to form necrosomes. Taken together, the cytotoxicity and immunoblotting results for **1** supports the notion that **1** induces necroptotic osteosarcoma cell death.

Co-incubation of **1** with the apoptosis inhibitor, z-VAD-FMK (5 µM),[31] resulted in a reduction in the potency of **1** towards U2OS cells (Figure 3, S4), however, this decrease in potency was statistically insignificant ($p > 0.05$) (Figure 3, S4). The cytotoxicity of cisplatin (an apoptosis-inducing platinum(II) complex) towards U2OS cells decreased significantly ($p < 0.05$) when co-incubated with z-VAD-FMK (Figure S8, S9). Immunoblotting studies indicated that proteins related to the apoptosis signaling pathway, such as cleaved caspases 3, 7 and poly ADP ribose polymerase (PARP-1) were observed at detectable levels in U2OS cells treated with **1** (20 µM for 72 h; Figure S7). Collectively, this shows that apoptosis may be occurring concurrently with necroptosis (in **1**-treated osteosarcoma cells), but to a smaller extent.

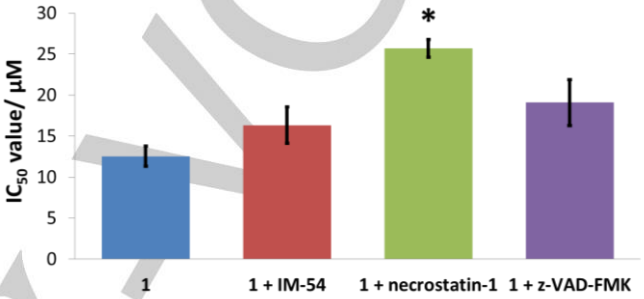

Figure 3. Graphical representation of the IC_{50} values of **1** against U2OS cells in the absence and presence of IM-54 (10 µM) or necrostatin-1 (20 µM) or z-VAD-FMK (5 µM). Error bars represent SD and Student t-test, * = $p < 0.05$.

Necroptosis features in osteosarcoma cells

Having found that RIP1-mediated necrosome formation is a likely prerequisite for **1** activity, we sought to understand how necrosome assembly leads to cell death. Necrosomes have been shown to induce necroptotic cell death through mitochondrial membrane dysfunction.[32] We used the JC-1 assay (5,5′,6,6′-tetrachloro-1,1′,3,3′-tetraethylbenzimidazolylcarbocyanine iodide) to probe the effect of **1** on the mitochondrial membrane potential of U2OS cells. JC-1 is green light emitting (*ca.* 529 nm) in its monomeric form and red light emitting (*ca.* 590 nm) in its aggregate form.[33] In healthy cells, JC-1 gathers in mitochondria forming aggregates (red), and in unhealthy cells (with mitochondrial membrane disruption) JC-1 forms monomers (green). Therefore, mitochondrial membrane depolarisation in a given cell population can be gauged by monitoring the red-green fluorescence intensity ratio. Upon treatment of U2OS cells with **1** (20 µM for 48 h) a noticeable increase (+15.6 %) in the proportion of cells exhibiting mitochondrial membrane depolarisation was detected by flow cytometric studies (Figure 4). A comparable effect was detected for U2OS cells treated with carbonyl cyanide *m*-chlorophenyl hydrazone (CCCP) (5 µM for 48 h), an established mitochondrial membrane depolariser, and shikonin (5 µM for 48 h) (Figure 4). Upon conducting the JC-1 assay for **1** and shikonin in the presence of necrostatin-1 (20 µM), the ability of **1** and shikonin to induce mitochondrial membrane depolarisation was reduced (Figure 4), indicating that both **1**- and shikonin-mediated mitochondrial membrane dysfunction is associated to necrosome formation.

Cells undergoing necroptosis exhibit specific morphological changes such as plasma membrane permeabilisation.[34] To confirm that **1** triggers morphological changes consistent with necroptosis, propidium iodide (PI)

staining studies were carried out using flow cytometric methods. PI is a dye that only penetrates and stains necrotic cells (with damaged cell membranes) in the absence of supplementary permeabilisation agents. PI is unable to stain early-stage apoptotic cell bodies as they tend to conserve their cell membrane structures. PI was readily taken up by U2OS cells dosed with **1** (20 μM for 72 h) compared to untreated control cells, indicative of **1**-induced necrosis (Figure 5). A comparable effect was also seen for U2OS cells dosed with shikonin (5 μM for 72 h) (Figure 5). Upon conducting the PI staining studies for **1**- and shikonin-treated U2OS cells in the presence of necrostatin-1 (20 μM), the ability of **1** and shikonin to induce PI staining was reduced (Figure 5). This implies that **1**-mediated plasma membrane permeabilisation is linked to necrosome formation.

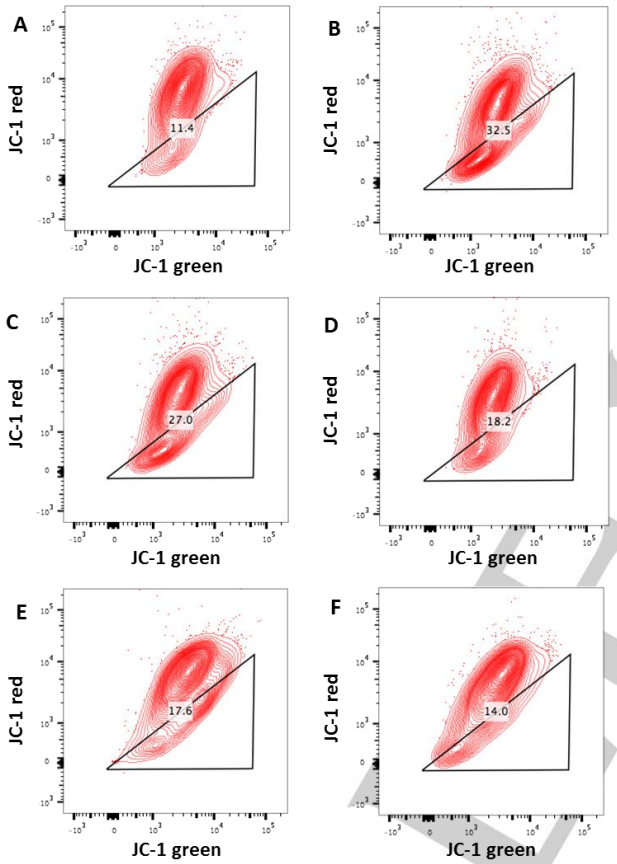

Figure 4. Representative 2D plots displaying the fluorescence emitted by JC-1 aggregates (red) and JC-1 monomers (green) by (A) untreated U2OS cells, (B) U2OS cells treated with CCCP (5 μM for 48 h), (C) U2OS cells treated with **1** (20 μM for 48 h), (D) U2OS cells treated with **1** (20 μM for 48 h) and nectrostatin-1 (20 μM for 48 h), (E) U2OS cells treated with shikinon (5 μM for 48 h), (F) U2OS cells treated with shikinon (5 μM for 48 h) and nectrostatin-1 (20 μM for 48 h). The marked area indicates the population of U2OS cells displaying mitochondrial membrane depolarisation.

Necroptosis independent of intracellular ROS elevation and PARP-1 activity

Intracellular reactive oxygen species (ROS) elevation is linked to cell death induced by the assembly of necrosomes.[35] To investigate whether osteosarcoma cell death induced by **1** is related to ROS elevation, the intracellular ROS level was monitored using a ROS indicator, 6-carboxy-2',7'-dichlorodihydrofluorescein diacetate (DCFH-DA). The intracellular ROS level in U2OS cells dosed with **1** (20 μM for 48 h) did not markedly change with respect to untreated cells (Figure S10). U2OS cells treated with the positive control, H_2O_2 (6 μM for 48 h) showed significantly higher levels of ROS ($p < 0.05$) compared to untreated cells (Figure S10). H_2O_2-induced ROS elevation in U2OS cells was reduced in the presence of the ROS scavenger, *N*-acetylcysteine (1.5 mM) (Figure S10). Collectively, this implies that **1**-induced cell death is not related to ROS elevation. In contrast, an elevated intracellular ROS level is a feature of shikonin-induced necroptosis in various cancer cell types.[36]

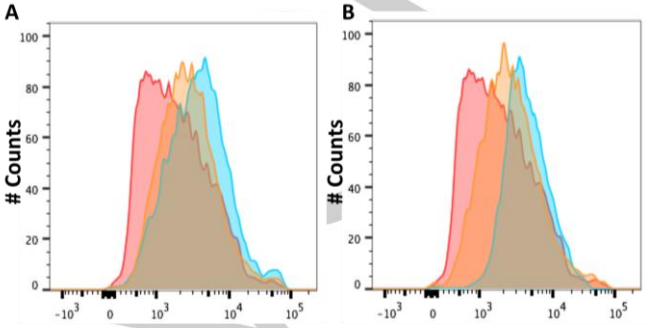

Figure 5. (A) Representative histograms displaying the fluorescence emitted by PI stained U2OS cells (red), or U2OS cells treated with **1** (20 μM for 72 h) (blue) or **1** (20 μM for 72 h) with nectrostatin-1 (20 μM for 72 h) (orange). (B) Representative histograms displaying the fluorescence emitted by PI stained U2OS cells (red), or U2OS cells treated shikonin (5 μM for 12 h) (blue) or shikonin (5 μM for 12 h) with nectrostatin-1 (20 μM for 72 h) (orange).

Hyperactivation of PARP-1, a chromatin-linked enzyme, which alters nuclear proteins by poly(ADP-ribosyl)ation, can also trigger necroptosis.[37] Bioenergetics related cell death can occur due to overactive PARP-1, which depletes ATP and NAD levels. PARP-1 hyperactivation can lead to necrosome formation and thus necroptotic cell death.[38] Cytotoxicity studies were carried out to probe whether **1**-mediated osteosarcoma cell death was related to PARP-1 activation. Specifically, the potency of **1** towards U2OS cells was measured in the presence of veliparib (ABT-888, 10 μM)[39] and 4-amino-1,8-naphthalimide (ANA, 10 μM),[40] both well-known PARP-1 inhibitors. The change in potency of **1** in the presence of ABT-888 and ANA was not statistically significant ($p > 0.05$) (Figure S11, S12). Therefore, this indicates that **1**-induced osteosarcoma cell death is not reliant on PARP-1 activity. In contrast, TRAIL (tumor necrosis factor (TNF)-related apoptosis inducing ligand)-and glutamate-induced necroptosis in various cancer cell types have been shown to be PARP-1 dependent.[37b,41] Cytotoxicity studies conducted with cisplatin (a chemical agent known to activate PARP-1)[42] showed that the potency of cisplatin towards U2OS cells was significantly ($p < 0.05$) attenuated when co-treated with ABT-888 and ANA (Figure S13, S14).

Conclusion

In summary, we show that the nickel(II)-phenanthroline-dithiocarbamate complex, **1** kills bulk osteosarcoma cells and OSCs comparably at micromolar concentrations. Notably, the nickel complex, **1** displays similar or better OSC potency than cisplatin and carboplatin in monolayer and three-dimensional osteosarcoma cell cultures. Mechanistic studies suggest that **1** kills osteosarcoma cells by necroptosis, a programmed form of necrosis. Specifically, **1** induces necrosome-dependent mitochondrial membrane depolarisation and cell membrane

disruption. This is, in part, due to **1**-mediated upregulation of necrosome components, RIP1 and RIP3. Compounds such as **1** (that induce cell death via non-apoptotic pathways) could be crucial in overcoming OSCs, as apoptosis resistance is a defining characteristic of OSCs. Detailed biological analysis shows that the necroptosis pathway evoked in osteosarcoma cells by **1** is distinctly different from that induced by shikonin, TRAIL, and glutamate (established necroptosis-inducing agents) in various cancer cell types. Unlike shikonin, **1** does not induce necroptosis by increasing intracellular ROS levels, and unlike TRAIL and glutamate, **1** does not induce necroptosis by promoting PARP-1 activity. Cancer cells (including osteosarcoma cells) can theoretically evolve necroptosis resistance by upregulating intracellular ROS scavengers or downregulating PARP-1 expression, thus necroptosis-inducers that act independently of ROS induction and PARP-1 activity are less prone to resistance. Given the above it is evident that **1** displays highly desirable biological properties, as it not only evokes necroptosis which can help circumvent apoptosis resistance, but also induces an atypical necroptotic signalling cascade that may enable it to overcome necroptosis-resistant mechanisms. As far as we are aware, this is the first investigation into the anti-osteosarcoma and anti-OSC properties of a nickel-containing compound. Our results strengthen and highlight the anticancer potential of nickel compounds, and more specifically encourages the development and progress of other nickel-containing compounds as necroptosis-inducing, anti-osteosarcoma agents.

Experimental Section

Materials and Methods. The nickel(II) complex, [Ni(*N*,*N*-diethyldithiocarbamate)$_2$(1,10-phenanthroline)], **1** was prepared and characterised using a reported protocol.[23] The purity of the nickel(II) complex, **1** was confirmed by elemental analysis [Anal. Calcd. for **1**, $C_{22}H_{28}N_4NiS_4$ (%): C, 49.35; H, 5.27; N, 10.46. Found: C, 49.18; H, 5.04; N, 10.41]. For all biological studies, the concentration of **1** was based on nickel concentration.

Cell Lines and Cell Culture Conditions. The U2OS bone osteosarcoma cell line and the HEK 293T embryonic kidney cell line were acquired from American Type Culture Collection (ATCC, Manassas, VA, USA) and cultured in Dulbecco's Modified Eagle's Medium (DMEM) supplemented with 1% penicillin and 10% fetal bovine serum. The cells were grown at 310 K in a humidified atmosphere containing 5% CO_2. To gain access to osteosarcoma stem cell (OSC)-enriched cells, a full T75 flask of U2OS cells was treated with methotrexate (300 nM) for 4 days. The cells (labelled U2OS-MTX cells) were used immediately. U2OS-MTX cells were characterised according to CD117 expression using flow cytometry as previously reported.[10]

Cytotoxicity MTT assay. The colourimetric MTT assay was used to determine the toxicity of **1**. U2OS, U2OS-MTX, or HEK 293T cells (5 × 10^3) were seeded in each well of a 96-well plate. After incubating the cells overnight, various concentrations of the compound (0.2-100 μM), was added and incubated for 72 h (total volume 200 μL). Stock solution of the compound was prepared as a 10 mM solution in DMSO and diluted using media. The final concentration of DMSO in each well was 0.5% and this amount was present in the untreated control as well. After 72 h, 20 μL of a 4 mg/mL solution of MTT in PBS was added to each well, and the plate was incubated for an additional 4 h. The DMEM/MTT mixture was aspirated and 200 μL of DMSO was added to dissolve the resulting purple formazan crystals. The absorbance of the solutions in each well was read at 550 nm. Absorbance values were normalized to (DMSO-containing) control wells and plotted as concentration of test compound versus % cell viability. IC_{50} values were interpolated from the resulting dose dependent curves. The reported IC_{50} values are the average of three independent experiments, each consisting of six replicates per concentration level (overall n = 18).

Sarcosphere Formation and Viability Assay. U2OS-MTX cells (5 × 10^3) were plated in ultralow-attachment 96-well plates (Corning) and incubated in DMEM/F12 medium supplemented with N2 (Invitrogen), human EGF (10 ng/mL), and human bFGF (10 ng/mL) for 10 days. Studies were also conducted in the presence of **1** and salinomycin (0-133 μM). Sarcospheres treated with **1** and salinomycin (at their respective IC_{20} values, 10 days) were imaged using an inverted microscope. The viability of the sarcospheres was determined by addition of a resazurin-based reagent, TOX8 (Sigma). After incubation for 16 h, the solutions were carefully transferred to a black 96-well plate (Corning), and the fluorescence of the solutions was read at 590 nm (λ_{ex} = 560 nm). Viable sarcospheres reduce the amount of the oxidized TOX8 form (blue) and concurrently increase the amount of the fluorescent TOX8 intermediate (red), indicating the degree of sarcosphere cytotoxicity caused by the test compound. Fluorescence values were normalized to DMSO-containing controls and plotted as concentration of test compound versus % sarcosphere viability. IC_{50} values were interpolated from the resulting dose dependent curves. The reported IC_{50} values are the average of three independent experiments, each consisting of three replicates per concentration level (overall n = 9).

Immunoblotting Analysis. U2OS cells (5 x 10^5 cells) were incubated with **1** (10-20 μM for 72 h at 37 ^oC. Cells were washed with PBS, scraped into SDS-PAGE loading buffer (64 mM Tris-HCl (pH 6.8)/ 9.6% glycerol/ 2% SDS/ 5% β-mercaptoethanol/ 0.01% Bromophenol Blue), and incubated at 95 ^oC for 10 min. Whole cell lysates were resolved by 4-20 % sodium dodecylsulphate polyacylamide gel electrophoresis (SDS-PAGE; 200 V for 25 min) followed by electro transfer to polyvinylidene difluoride membrane, PVDF (350 mA for 1 h). Membranes were blocked in 5% (w/v) non-fat milk in PBST (PBS/0.1% Tween 20) and incubated with the appropriate primary antibodies (Cell Signalling Technology). After incubation with horseradish peroxidase-conjugated secondary antibodies (Cell Signalling Technology), immune complexes were detected with the ECL detection reagent (BioRad) and analysed using a chemiluminescence imager (Bio-Rad ChemiDoc).

JC-1 Assay. The JC-1 Mitochondrial Membrane Potential Assay Kit (Cayman) was used. The manufacturer's protocol was followed to carry out this experiment. Untreated and treated U2OS cells (1 × 10^6 cells) grown in six-well plates were treated with the JC-1 staining solution (100 μL/mL of cell media). The cells were incubated for 30 min, harvested, and analysed using a FACSCanto II flow cytometer (BD Biosciences) (10,000 events per sample were acquired). The FL1 and FL2 channels were used to assess mitochondrial depolarisation. Cell populations were analysed using the FlowJo software (Tree Star).

Propidium Iodide (PI) Uptake. Untreated and treated U2OS cells (1 × 10^6 cells/well) grown in six-well plates were washed with PBS (1 mL × 3), harvested, incubated with PI (5 μM), and analysed by using a FACSCanto II flow cytometer (BD Biosciences) (10,000 events per sample were acquired). The FL2 channel was used to assess intracellular PI uptake. Cell populations were analysed using the FlowJo software (Tree Star).

Intracellular ROS Assay. U2OS cells (5 × 10^3) were seeded in each well of a 96-well plate. After incubating the cells overnight, they were treated with **1** or H_2O_2 (20 and 6 μM for 48 h), in the presence or absence of *N*-acetylcysteine (1.5 mM), and incubated with 6-carboxy-2′,7′-dichlorodihydrofluorescein diacetate (20 μM) for 30 min. The intracellular ROS level was determined by measuring the fluorescence of the solutions in each well at 529 nm (λ_{ex} = 504 nm).

Acknowledgements ((optional))

K.S. is supported by an EPSRC New Investigator Award (EP/S005544/1).

Keywords: nickel • cancer • necroptosis • osteosarcoma stem cells • bioinorganic chemistry

[1] R. L. Siegel, K. D. Miller, A. Jemal, *CA: Cancer J. Clin.* **2018**, *68*, 7-30.
[2] A. K. Raymond, *World Health Organization classification of tumours : pathology and genetics Tumours of Soft Tissue and Bone* **2002**, 264-270.

[3] American Cancer Society, **2020** Society, https://www.cancer.org/cancer/osteosarcoma/detection-diagnosis-staging/survival-rates.

[4] a) V. A. Siclari, L. Qin, *J. Orthop. Surg. Res.* **2010**, *5*, 78; b) G. N. Yan, Y. F. Lv, Q. N. Guo, *Cancer Lett.* **2016**, *370*, 268-274; c) H. K. Brown, M. Tellez-Gabriel, D. Heymann, *Cancer Lett.* **2017**, *386*, 189-195.

[5] a) U. Basu-Roy, C. Basilico, A. Mansukhani, *Cancer Lett.* **2013**, *338*, 158-167; b) U. Basu-Roy, E. Seo, L. Ramanathapuram, T. B. Rapp, J. A. Perry, S. H. Orkin, A. Mansukhani, C. Basilico, *Oncogene* **2012**, *31*, 2270-2282.

[6] a) S. Chumsri, A. M. Burger, *Curr. Opin. Mol. Ther.* **2008**, *10*, 323-333; b) S. R. Martins-Neves, D. I. Paiva-Oliveira, P. M. Wijers-Koster, A. J. Abrunhosa, C. Fontes-Ribeiro, J. V. Bovee, A. M. Cleton-Jansen, C. M. Gomes, *Cancer Lett.* **2016**, *370*, 286-295.

[7] a) A. Halldorsson, S. Brooks, S. Montgomery, S. Graham, *J. Med. Case Rep.* **2009**, *3*, 9298; b) A. He, W. Qi, Y. Huang, T. Feng, J. Chen, Y. Sun, Z. Shen, Y. Yao, *Exp. Ther. Med.* **2012**, *4*, 435-441.

[8] a) Q. L. Tang, Z. Q. Zhao, J. C. Li, Y. Liang, J. Q. Yin, C. Y. Zou, X. B. Xie, Y. X. Zeng, J. N. Shen, T. Kang, J. Wang, *Cancer Lett.* **2011**, *311*, 113-121; b) L. Peng, D. Jiang, *PloS one* **2018**, *13*, e0205918; c) W. Liu, Z. Zhao, Y. Wang, W. Li, Q. Su, Q. Jia, J. Zhang, X. Zhang, J. Shen, J. Yin, *Cell Death Dis.* **2018**, *9*, 343; d) H. Y. Xu, W. Fang, Z. W. Huang, J. C. Lu, Y. Q. Wang, Q. L. Tang, G. H. Song, Y. Kang, X. J. Zhu, C. Y. Zou, H. L. Yang, J. N. Shen, J. Wang, *Eur. Rev. Med. Pharmacol. Sci.* **2017**, *21*, 4516-4528.

[9] K. Laws, K. Suntharalingam, *ChemBioChem* **2018**, *19*, 2246-2253.

[10] P. Robin, K. Singh, K. Suntharalingam, *Chem. Commun.* **2020**, *56*, 1509-1512.

[11] a) D. Wang, S. J. Lippard, *Nat. Rev. Drug Discov.* **2005**, *4*, 307-320; b) U. Fischer, K. Schulze-Osthoff, *Cell Death Differ.* **2005**, *12 Suppl 1*, 942-961; c) J. A. Hickman, *Cancer Metastasis Rev.* **1992**, *11*, 121-139.

[12] a) C.-P. Tan, Y.-Y. Lu, L.-N. Ji, Z.-W. Mao, *Metallomics* **2014**, *6*, 978-995; b) M. J. Chow, M. Alfiean, G. Pastorin, C. Gaiddon, W. H. Ang, *Chem. Sci.* **2017**, *8*, 3641-3649.

[13] a) S. J. Dixon, K. M. Lemberg, M. R. Lamprecht, R. Skouta, E. M. Zaitsev, C. E. Gleason, D. N. Patel, A. J. Bauer, A. M. Cantley, W. S. Yang, B. Morrison, 3rd, B. R. Stockwell, *Cell* **2012**, *149*, 1060-1072; b) S. W. G. Tait, G. Ichim, D. R. Green, *J. Cell Sci.* **2014**, *127*, 2135-2144.

[14] T. Vanden Berghe, A. Linkermann, S. Jouan-Lanhouet, H. Walczak, P. Vandenabeele, *Nat. Rev. Mol. Cell Biol.* **2014**, *15*, 135-147.

[15] P. Vandenabeele, L. Galluzzi, T. Vanden Berghe, G. Kroemer, *Nat. Rev. Mol. Cell Biol.* **2010**, *11*, 700-714.

[16] a) Z. Cai, S. Jitkaew, J. Zhao, H. C. Chiang, S. Choksi, J. Liu, Y. Ward, L. G. Wu, Z. G. Liu, *Nat. Cell Biol.* **2014**, *16*, 55-65; b) S. Jouan-Lanhouet, F. Riquet, L. Duprez, T. Vanden Berghe, N. Takahashi, P. Vandenabeele, *Semin. Cell Dev. Biol.* **2014**, *35*, 2-13; c) J. Li, T. McQuade, A. B. Siemer, J. Napetschnig, K. Moriwaki, Y. S. Hsiao, E. Damko, D. Moquin, T. Walz, A. McDermott, F. K. Chan, H. Wu, *Cell* **2012**, *150*, 339-350.

[17] K. M. Irrinki, K. Mallilankaraman, R. J. Thapa, H. C. Chandramoorthy, F. J. Smith, N. R. Jog, R. K. Gandhirajan, S. G. Kelsen, S. R. Houser, M. J. May, S. Balachandran, M. Madesh, *Mol. Cell Biol.* **2011**, *31*, 3745-3758.

[18] Z. Su, Z. Yang, L. Xie, J. P. DeWitt, Y. Chen, *Cell Death Differ.* **2016**, *23*, 748-756.

[19] T. Fujiwara, T. Ozaki, *Stem Cells Int.* **2016**, *2016*, 2603092.

[20] V. Novohradsky, L. Markova, H. Kostrhunova, Z. Trávníček, V. Brabec, J. Kasparkova, *Sci. Rep.* **2019**, *9*, 13327.

[21] T. C. Johnstone, K. Suntharalingam, S. J. Lippard, *Chem. Rev.* **2016**, *116*, 3436-3486.

[22] A. S. Abu-Surrah, M. Kettunen, *Curr. Med. Chem.* **2006**, *13*, 1337-1357.

[23] M. Flamme, P. B. Cressey, C. Lu, P. M. Bruno, A. Eskandari, M. T. Hemann, G. Hogarth, K. Suntharalingam, *Chem. Eur. J.***2017**, *23*, 9674-9682.

[24] a) X. Zhang, J. H. Cui, Q. Q. Meng, S. S. Li, W. Zhou, S. Xiao, *Mini-Rev. Med. Chem.* **2018**, *18*, 164-172; b) W. Han, L. Li, S. Qiu, Q. Lu, Q. Pan, Y. Gu, J. Luo, X. Hu, *Mol. Cancer Ther.* **2007**, *6*, 1641-1649.

[25] Q. L. Tang, Y. Liang, X. B. Xie, J. Q. Yin, C. Y. Zou, Z. Q. Zhao, J. N. Shen, J. Wang, *Chin. J. Cancer* **2011**, *30*, 426-432.

[26] A. S. Adhikari, N. Agarwal, B. M. Wood, C. Porretta, B. Ruiz, R. R. Pochampally, T. Iwakuma, *Cancer Res.* **2010**, *70*, 4602-4612.

[27] K. Dodo, M. Katoh, T. Shimizu, M. Takahashi, M. Sodeoka, *Bioorg. Med. Chem. Lett.* **2005**, *15*, 3114-3118.

[28] a) A. Degterev, J. Hitomi, M. Germscheid, I. L. Ch'en, O. Korkina, X. Teng, D. Abbott, G. D. Cuny, C. Yuan, G. Wagner, S. M. Hedrick, S. A. Gerber, A. Lugovskoy, J. Yuan, *Nat. Chem. Biol.* **2008**, *4*, 313-321; b) A. Degterev, Z. Huang, M. Boyce, Y. Li, P. Jagtap, N. Mizushima, G. D. Cuny, T. J. Mitchison, M. A. Moskowitz, J. Yuan, *Nat. Chem. Biol.* **2005**, *1*, 112-119.

[29] a) G.-B. Koo, M. J. Morgan, D.-G. Lee, W.-J. Kim, J.-H. Yoon, J. S. Koo, S. I. Kim, S. J. Kim, M. K. Son, S. S. Hong, J. M. M. Levy, D. A. Pollyea, C. T. Jordan, P. Yan, D. Frankhouser, D. Nicolet, K. Maharry, G. Marcucci, K. S. Choi, H. Cho, A. Thorburn, Y.-S. Kim, *Cell Res.* **2015**, *25*, 707-725; b) M. J. Morgan, Y. S. Kim, *BMB Rep.* **2015**, *48*, 303-312.

[30] Z. Fu, B. Deng, Y. Liao, L. Shan, F. Yin, Z. Wang, H. Zeng, D. Zuo, Y. Hua, Z. Cai, *BMC cancer* **2013**, *13*, 580.

[31] E. A. Slee, H. Zhu, S. C. Chow, M. MacFarlane, D. W. Nicholson, G. M. Cohen, *Biochem. J.* **1996**, *315 (Pt 1)*, 21-24.

[32] a) S. He, L. Wang, L. Miao, T. Wang, F. Du, L. Zhao, X. Wang, *Cell* **2009**, *137*, 1100-1111; b) V. Temkin, Q. Huang, H. Liu, H. Osada, R. M. Pope, *Mol. Cell Biol.* **2006**, *26*, 2215-2225.

[33] S. T. Smiley, M. Reers, C. Mottola-Hartshorn, M. Lin, A. Chen, T. W. Smith, G. D. Steele, Jr., L. B. Chen, *Proc. Natl. Acad. Sci. U.S.A.* **1991**, *88*, 3671-3675.

[34] a) M. C. de Almagro, D. Vucic, *Semin. Cell Dev. Biol.* **2015**, *39*, 56-62; b) A. Oberst, *FEBS J.* **2016**, *283*, 2616-2625.

[35] a) Y. S. Cho, S. Challa, D. Moquin, R. Genga, T. D. Ray, M. Guildford, F. K. Chan, *Cell* **2009**, *137*, 1112-1123; b) C. W. Davis, B. J. Hawkins, S. Ramasamy, K. M. Irrinki, B. A. Cameron, K. Islam, V. P. Daswani, P. J. Doonan, Y. Manevich, M. Madesh, *Free Radic. Biol. Med.* **2010**, *48*, 306-317; c) D. W. Zhang, J. Shao, J. Lin, N. Zhang, B. J. Lu, S. C. Lin, M. Q. Dong, J. Han, *Science* **2009**, *325*, 332-336.

[36] a) C. Huang, Y. Luo, J. Zhao, F. Yang, H. Zhao, W. Fan, P. Ge, *PloS one* **2013**, *8*, e66326; b) Z. Shahsavari, F. Karami-Tehrani, S. Salami, *Asian Pac. J. Cancer Prev.* **2015**, *16*, 7261-7266; c) T. Liu, X. Sun, Z. Cao, *Onco. Targets Ther.* **2019**, *12*, 2605-2614; d) B. Lu, X. Gong, Z.-q. Wang, Y. Ding, C. Wang, T.-f. Luo, M.-h. Piao, F.-k. Meng, G.-f. Chi, Y.-n. Luo, P.-f. Ge, *Acta Pharmacol. Sin.* **2017**, *38*, 1543-1553.

[37] a) J. Sosna, S. Voigt, S. Mathieu, A. Lange, L. Thon, P. Davarnia, T. Herdegen, A. Linkermann, A. Rittger, F. K. Chan, D. Kabelitz, S. Schutze, D. Adam, *Cell Mol. Life. Sci.* **2014**, *71*, 331-348; b) X. Xu, C. C. Chua, M. Zhang, D. Geng, C. F. Liu, R. C. Hamdy, B. H. Chua, *Brain Res.* **2010**, *1343*, 206-212.

[38] R. Chavez-Valdez, L. J. Martin, F. J. Northington, *Neurol. Res. Int.* **2012**, *2012*, 257563.

[39] C. K. Donawho, Y. Luo, Y. Luo, T. D. Penning, J. L. Bauch, J. J. Bouska, V. D. Bontcheva-Diaz, B. F. Cox, T. L. DeWeese, L. E. Dillehay, D. C. Ferguson, N. S. Ghoreishi-Haack, D. R. Grimm, R. Guan, E. K. Han, R. R. Holley-Shanks, B. Hristov, K. B. Idler, K. Jarvis, E. F. Johnson, L. R. Kleinberg, V. Klinghofer, L. M. Lasko, X. Liu, K. C. Marsh, T. P. McGonigal, J. A. Meulbroek, A. M. Olson, J. P. Palma, L. E. Rodriguez, Y. Shi, J. A. Stavropoulos, A. C. Tsurutani, G. D. Zhu, S. H. Rosenberg, V. L. Giranda, D. J. Frost, *Clin. Cancer Res.* **2007**, *13*, 2728-2737.

[40] M. Banasik, H. Komura, M. Shimoyama, K. Ueda, *J. Biol. Chem.* **1992**, *267*, 1569-1575.

[41] S. Jouan-Lanhouet, M. I. Arshad, C. Piquet-Pellorce, C. Martin-Chouly, G. Le Moigne-Muller, F. Van Herreweghe, N. Takahashi, O. Sergent, D. Lagadic-Gossmann, P. Vandenabeele, M. Samson, M. T. Dimanche-Boitrel, *Cell Death Differ.* **2012**, *19*, 2003-2014.

[42] S. Park, S. P. Yoon, J. Kim, *Anat. Cell Biol.* **2015**, *48*, 66-74.

Entry for the Table of Contents

Insert graphic for Table of Contents here. ((Please ensure your graphic is in **one** of following formats))

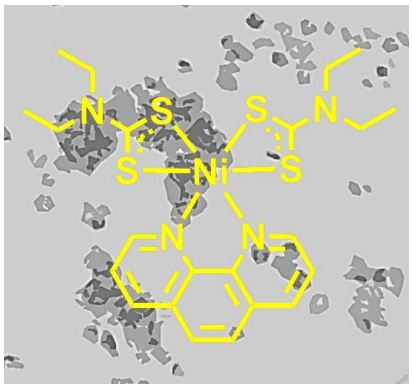

Osteosarcoma is the most prevalent primary bone cancer amongst adults and children. A nickel(II) coordination complex containing one 1,10-phenanthroline ligand and two *N*,*N*-diethyldithiocarbamate moieties is shown to kill osteosarcoma cells by necroptosis, an ordered form of necrosis. Encouragingly, the nickel complex kills bulk osteosarcoma cells and hard-to-kill osteosarcoma stem cell (OSC) comparably at micromolar concentrations.

Institute and/or researcher Twitter usernames: @_Suntharalingam @eskandari_arvin @Leicesterchem @LeiStructBio